Characterization of the Martian Surface Layer

GERMÁN MARTÍNEZ, FRANCISCO VALERO, AND LUIS VÁZQUEZ

Universidad Complutense de Madrid, Madrid, Spain

(Manuscript received 20 February 2008, in final form 12 May 2008)

ABSTRACT

The authors have estimated the diurnal evolution of Monin–Obukhov length, friction velocity, temperature scale, surface heat flux, eddy-transfer coefficients for momentum and heat, and turbulent viscous dissipation rate on the Martian surface layer for a complete sol belonging to the Pathfinder mission. All these magnitudes have been derived from in situ wind and temperature measurements at around 1.3-m height and simulated ground temperature (from 0600 sol 25 to 0600 sol 26). Previously, neither values of turbulent viscous dissipation rate and eddy-transfer coefficients from in situ measurements for the Martian surface layer nor diurnal evolutions of all the previously mentioned turbulent parameters for the Pathfinder had been obtained.

Monin–Obukhov similarity theory for stratified surface layers has been applied to obtain the results. The values assigned to the surface roughness and the applied parameterization of the interfacial sublayer will be discussed in detail with respect to the results' sensitivity to them.

The authors have found similarities concerning the order of magnitude and qualitative behavior of Monin–Obukhov length, friction velocity, and turbulent viscous dissipation rate on Earth and on Mars. However, quantities directly related to the lower Martian atmospheric density and thermal inertia, like temperature scale and hence surface heat flux, range over different orders of magnitude. Additionally, turbulent exchanges in the first few meters have been found to be just two orders of magnitude higher than the molecular ones, whereas on Earth around five orders of magnitude separate both mechanisms.

1. Introduction

The planetary boundary layer (PBL) can be defined as that part of the atmosphere that is directly influenced by the presence of the planet surface and responds to surface forcings with a time scale of ~1 hr or less. Belonging to the PBL, the surface layer is the region at the bottom of the PBL where turbulent fluxes and stress vary by less than 10% of their magnitude (Stull 1988). The sharpest variations in meteorological magnitudes take place in this layer and, consequently, so do the most significant exchanges of momentum, heat, and mass (Arya 2001).

The study of the Martian surface layer (MSL) becomes essential for two reasons. The first one concerns practical issues. Topics like variation rates of a magnitude associated with a concrete process (such as the sampling rate required to capture a phenomenon) are needed for the design of the sensors. The second reason lies in the feedback between different scale processes. Phenomena with different time scales are interrelated, just as on Earth. That is, the dynamic of the MSL affects mesoscale and synoptic phenomena, whose characterizing time scales are larger, and the reverse is also true. Consequently, understanding all time scale phenomena is necessary for a better understanding of any of them.

Research concerning the MSL involves significant drawbacks associated with the lack of suitable data. Only the Viking and Pathfinder (PF) missions have provided in situ suitable meteorological data (high-resolution temperature vertical profiles have been monitored by the Mars Exploration Rover, although these data are not yet available). Viking landers (Hess et al. 1977) measured pressure, wind, and temperature at one height with a maximum sampling rate of about 0.8 Hz, used during periods spanning around 1 h. On the other hand, the PF lander (Schofield et al. 1997) measured pressure at one height and temperature at three different heights, with a nominal sampling rate of

Corresponding author address: Germán Martínez, Dept. de Ciencias de la Atmósfera y Astrofísica II, Facultad de Física, Universidad Complutense de Madrid, Av. Complutense s/n, Madrid, MA 28040, Spain.
E-mail: mmgerman@fis.ucm.es

DOI: 10.1175/2008JAS2765.1

0.25 Hz and a maximum sampling rate of 1 Hz for periods not longer than 1 h. Unfortunately, the wind sensor experienced problems and wind data are not available in the Planetary Data Science dataset.

Seminal works have been written despite these sparse in situ data. Sutton et al. (1978) showed the diurnal behavior of Monin–Obukhov length, friction velocity, and surface heat flux for the first 45 sols (1 sol corresponds to 1 Martian day, approximately 24.7 h) based on wind and temperature data measured by the Viking landers. Some years after, Savijärvi (1991) developed a one-dimensional boundary layer model that simulated the diurnal behavior of the surface heat flux for the Viking mission and was also used to compare in situ Viking data (wind, temperature, and vertical profiles during the entry) to the outputs of the model. Another one-dimensional boundary layer model, in which the diurnal evolution of surface heat flux and friction velocity for the first sols of the Viking mission were simulated, was developed by Haberle et al. (1993). Wind and temperature spectra from in situ wind and temperature measurements were carried out by Tillman et al. (1994) for the Viking mission. In that paper, the Monin–Obukhov length diurnal evolution for 1 day was shown as well as values for specific hours of friction velocity and surface heat flux. Savijärvi (1999) and Määttänen and Savijärvi (2004) estimated values of Monin–Obukhov length and eddy-diffusion coefficients and simulated the diurnal evolution of surface heat flux for the PF mission based on the Savijärvi one-dimensional boundary layer model (Savijärvi 1991). Larsen et al. (2002) carried out research similar to that of Tillman et al. (1994) and studied the wind and temperature spectra for the PF mission from in situ wind and temperature measurements for specific hours, although neither diurnal evolutions nor single values of Monin–Obukhov length, friction velocity, or temperature scale were given.

Sutton et al. (1978), Tillman et al. (1994), and Larsen et al. (2002), who used in situ wind and temperature data, needed the help of Monin–Obukhov similarity theory to yield diurnal evolutions of turbulent parameters. The reason relies on two facts. First, vertical wind components have never been measured on Mars; second, even if they had been measured, turbulent parameters like friction velocity and temperature scale would have not been accurately obtained by the covariance method because of the low sampling rate used. As a consequence, turbulent magnitudes on Mars can only be obtained from mean variables (by mean variables we refer to 1-h averaged values). And this is exactly the modus operandi of Monin–Obukhov similarity theory and the reason why this theory is widely used in the research of the MSL.

It can be noticed that no diurnal evolution of turbulent parameters from in situ data has been reported in the above mentioned literature for the PF mission. The main reason is a problem experienced by the wind sensor, because of which wind data are not available in the Planetary Data Science dataset. However, we have recently received quality controlled wind data for a complete sol with a sampling rate of 0.25 Hz, covering from 0600 sol 25 to 0600 sol 26 [in situ PF wind data corresponding to other sols, in which measurements did not cover the whole day continuously, have been used by other authors, including Larsen et al. (2002), Määttänen and Savijärvi (2004), and Savijärvi et al. (2004)].

These in situ wind data, in situ temperatures (measured at the top height of the lander mast), and hourly simulated ground temperatures obtained from the one-dimensional boundary layer model (Savijärvi et al. 2004) form the input for this work. From them, the diurnal evolution of the main turbulent parameters for the PF landing area has been obtained. The Monin–Obukhov length, friction velocity, and temperature scale (and consequently the surface heat flux, whose diurnal evolutions had already been obtained for the Viking mission from in situ measurements) will be shown for the PF in this paper. Finally, we have derived the daily behavior of turbulent viscous dissipation rate and eddy diffusion coefficients whose values had not previously been available from in situ measurements for the MSL.

The inputs, especially wind data, will be discussed in section 2. Section 3 is divided into two parts. We shall study the applicability of the Monin–Obukhov similarity theory for stratified surface layers on Mars first, and then the method employed to derive the results will be described. Issues related to the value of the surface roughness and the parameterization of the interfacial sublayer will be emphasized. In section 4, we will show diurnal evolutions of all the parameters under study for the different proposed values of the surface roughness. Moreover, those parameters that are sensitively affected by the inclusion of the interfacial sublayer will be shown separately to explain how they change. Section 4 closes with a comparison between the Martian results obtained here and their known terrestrial counterparts to highlight the main differences between the planets. Finally, we will summarize the main conclusions in section 5.

2. Data

Three sets of data form the inputs of this paper: in situ observed wind and temperature measurements and

simulated ground temperature, all covering from 0600 sol 25 to 0600 sol 26 of the PF mission (the period of study, or PS). Before explaining the characteristics of each separately, a brief summary of the PF mission will be given.

The PF lander touched down on 4 July 1997 at 19.7°N, 33.55°W in the Ares Vallis region of Chryse Planitia. It was northern summer at this time, corresponding to a solar longitude of about 140°. The total duration of the mission was 83 sols, although sols 17, 31, 43, 45, 46, 48, and 51 contained no meteorology data. Through the other 76 sols, pressure at one height and temperature at three different heights were properly collected by the Meteorology Package Instrument; however, the wind portion of the system design was flawed. Continuous sampling for a complete sol at 0.25 Hz was conducted on sols 25, 32, 38, 55, and 68; the nominal strategy consisted of measuring 51 equally spaced times for 3 min during the first 30 sols. During the extended mission (sols 31–83) the Meteorology Package Instrument data were monitored inside the hours 0900–1500 local solar time (LST).

Because the accuracy of the results depends on the reliability of the inputs, we review them here, starting with wind data. The PF wind sensor experienced problems related to overheating of the sensor wire segments used to derive wind speed. The lack of a representative temperature that could serve as a baseline against which overheating could be determined caused the failure. Thermocoupled gas-temperature measurements have been used as an alternative to provide a valid representation of unheated wire temperatures.

In this way, wind data monitored with a sampling rate of 0.25 Hz covering the PS have been provided. The main uncertainties of the derived wind data are concentrated over the daytime because of the short-term large temperature fluctuation, whereas from around 5 p.m. to 6 a.m., when strong stability makes temperature fluctuations small, wind speed data are more reliable. Figure 1 shows the 1-h averaged wind data at a height of 1.09 m above the lander petals (i.e., around 1.30 m above the ground). As the local instability increases, convection gets stronger, mixing the air at 1.3 m with air from above where wind velocity is higher. The result is the peak observed around 0400 (see Fig. 1). This behavior and the magnitude of the wind match with those found in Viking mission and with those occurring on Earth.

The second observed maximum is supposed to be related to the frictional decoupling caused by the mixed layer collapse after sunset. The formed Martian nocturnal low-level jet (Savijärvi and Siili 1993) would create a high turbulent kinetic energy layer which, through a shear mechanism (expected to be very important because of the strong nighttime inversions), could propagate downward. The result would be this local maximum, which can also be observed in Savijärvi et al. (2004).

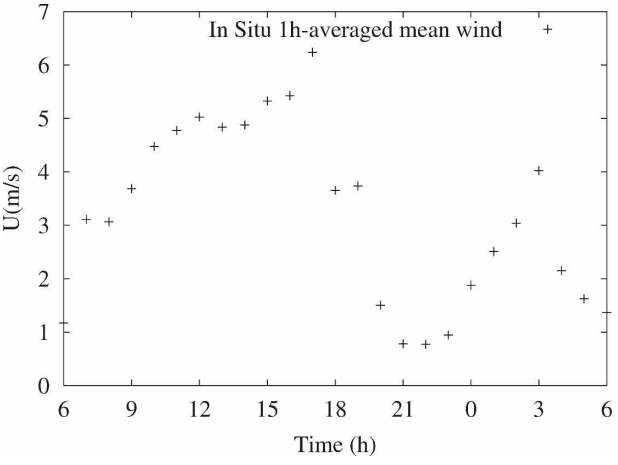

FIG. 1. Diurnal evolution of the 1-h averaged wind speed for sols 25–26 from the Pathfinder lander.

We now turn to temperature measurements. Temperature was monitored at three different heights on the mast of the PF lander. The top height (1.27 m) temperature has been used in this work for two reasons: it is likely to be less contaminated by the thermal radiation of the lander, and the height virtually matches the wind sensor height (about 1.30 m), which is required for the employed methodology. The sampling rate used was 0.25 Hz during the PS, as for wind. We represent the 1-h averaged temperature in Fig. 2. The diurnal temperature behavior is quite typical because the sol-to-sol temperatures have been very repeatable over the first 30 sols (Larsen et al. 2002). The maximum temperature, about 260 K, is reached between 1400 and 1500 LST. The minimum, around 195 K, is observed by 0500, just before sunrise.

To close the characterization of the inputs, simulated ground temperature is now discussed. A one-dimensional boundary layer model (Savijärvi et al. 2004), kindly shared by Prof. Savijärvi, has been used to estimate hourly outputs of ground temperature during the PS. In this paper, this model has been slightly modified and values of 0.19 and 387 J m^{-2} K^{-1} $s^{-1/2}$ for albedo and thermal inertia, respectively, have been used to run the model and to create the most probable scenario for the ground temperature (see Fig. 2). In addition, two other extreme scenarios, the warmest and the coldest, have been created by using extreme reliable values of surface emissivity (Christensen et al. 2001), dust optical depth (Johnson et al. 2003), and finally albedo and ther-

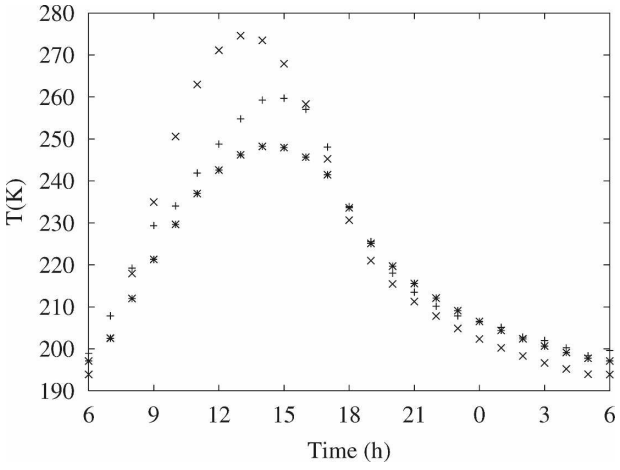

FIG. 2. The figure shows three diurnal evolutions of temperature for sols 25–26: the 1-h averaged in situ temperature at 1.27 m (+), the simulated temperature at the same height (*), and the simulated ground temperature (×).

mal inertia (Putzig et al. 2005) for the PF location. In situ temperature measurements at the bottom height have also been considered for creating such scenarios. They have been used as a lower limit for the ground temperature during the daytime and as an upper limit at night. As a result, ground temperature has been reduced by 4 and 3 K during the nighttime and daytime respectively in the coldest scenario, whereas the warmest temperatures have increased by 8 K during the daytime and around 2 K at night. The sensitivity of the results to these limiting cases will be discussed later.

It is worthwhile to mention that even though only one day has been used, it is highly expected to represent a typical day of the northern summer for the PF landing region because of the very small influence of atmospheric distortion and variability over the first 30 sols.

In summary, 900 observed wind and temperature data, corresponding to ±30 min (at a 0.25 Hz sampling rate) from each specific hour, have been averaged to yield hourly inputs from 0600 sol 25 to 0600 sol 26. By employing this time average, long-term trends are filtered and only turbulence is expected to remain (Stull 1988). Thus, 25 hourly inputs both for temperature and wind and 25 simulated ground temperatures hourly inputs have been used to compute the values of the turbulent parameters obtained.

3. Methodology

The previously mentioned dataset, *K*-theory, and Monin–Obukhov similarity theory for stratified surface layers will be used to estimate the diurnal behavior of Monin–Obukhov length L, friction velocity u_*, temperature scale T_*, dynamic surface heat flux H_0, turbulent viscous dissipation rate ϵ, and eddy diffusivity coefficients for momentum k_m and heat k_h.

Before showing in detail the method employed to derive the results, a brief explanation of the applicability of the similarity theory for stratified surface layers on Mars will be given.

a. On the applicability of the similarity theory on Mars

To employ the similarity theory some hypotheses should be accepted. We shall enumerate these hypotheses and explain to what extent they agree on Mars.

Assuming a horizontally homogeneous and quasi-stationary surface layer in which turbulent fluxes are not dependent on height, and assuming that both the Coriolis effect and molecular exchanges are neglected, magnitudes concerning the mean flow and turbulent characteristics depend only on four independent variables: the buoyancy parameter g/T_g, the height above the ground z, the surface drag or equivalent friction velocity $u_* = \sqrt{|\tau_0|/\rho}$, and the kinematic surface heat flux $H_0/\rho c_p$ (Monin and Obukhov 1954). Because these four variables involve only three fundamental dimensions, the Buckingham pi theorem states that only one dimensionless parameter can be formed, $\varsigma = z/L$, where

$$L = -\frac{u_*^3}{k\dfrac{g}{T_g}\dfrac{H_0}{\rho c_p}}$$

is the Monin–Obukhov length. In addition, any other dependent variable, when made dimensionless by the fundamental scales z, u_*, and $T_* = -H_0/\rho c_p u_*$ (formed with three of the independent variables), is a unique function of $\zeta = z/L$.

We shall treat separately each of the required hypotheses to use the similarity theory on Mars. The complexity of the terrain, along with large-scale phenomena (synoptic perturbations), can greatly alter horizontal homogeneity. However, synoptic perturbations were not present at the time and location of the study, and the landing site, although not especially flat, did not present a sharp topography (Golombek et al. 1997). On the other hand, in this work we have found molecular exchanges to be two orders of magnitude lower than turbulent diffusion in the first few meters, which still allows us to neglect molecular diffusion in the surface layer. Moreover, the height of the surface layer and the magnitude of the Coriolis force are found to be of the same order as on Earth; consequently, the Coriolis force can be neglected. Concerning the suspended dust, similarity theory does not take into account this Mar-

tian phenomenon (note that neither of the independent variables takes direct notice of dust). Nevertheless, the observed dustiness was low (Savijärvi 1999) and the importance of the dust was reduced. Finally, the analytical form in which any dimensionless variable depends on the dimensionless parameter $\zeta = z/L$ (e.g., the universal functions for momentum and heat) has been supposed to be the same as on Earth.

b. The bulk method: Universal functions, roughness length, and the interfacial sublayer

The method employed to obtain the results will be explained in this section. In addition, the values assigned to the surface roughness length z_0, the inclusion of the interfacial sublayer (that layer of air in which the transfer of momentum and heat is dominated by molecular processes), and the analytical form of the universal functions for heat and momentum will be carefully described.

Because of the nature of the inputs, the bulk method (Arya 2001) has been used. Mean wind and mean temperature measured at the same height (we will suppose the same height for wind and temperature measurements because only about 3 cm separate them) as well as ground temperature are needed by this method. Following this approach, the bulk Richardson number can be written as

$$R_B = \frac{g}{T_g}\frac{(T - T_g)z}{U^2}, \tag{1}$$

where g is the Martian surface gravity (=3.7 m s^{-2}), T_g is the surface temperature, and z is the height where wind U and temperature T have been monitored. Several hypotheses have been taken into account to derive the analytical form of (1): the mean wind has been supposed to be aligned with the x axis, subsidence has been neglected, virtual potential temperature has been substituted for the standard temperature (Tillman et al. 1994), and turbulent fluxes of momentum $\overline{u'w'}$ and heat $\overline{w'T'}$ have been parameterized with equal diffusion coefficients ($k_m = k_h$) via K-theory:

$$\overline{u'w'} = -k_m\frac{\partial U}{\partial z} \quad \text{and} \tag{2}$$

$$\overline{w'T'} = -k_h\frac{\partial T}{\partial z}. \tag{3}$$

Substituting $T - T_g$ and U^2 into (1) from the integration of the similarity relationships—

$$\frac{kz}{u_*}\frac{\partial U}{\partial z} = \phi_m(\zeta) \quad \text{and} \tag{4}$$

$$\frac{kz}{T_*}\frac{\partial T}{\partial z} = \phi_h(\zeta) \tag{5}$$

leads to

$$\frac{g}{T_g}\frac{(\overline{T} - T_g)z}{\overline{U}^2} = \zeta\frac{\displaystyle\int_{\zeta_{0T}}^{\zeta}\zeta'^{-1}\phi_h(\zeta')\,d\zeta'}{\left[\displaystyle\int_{\zeta_0}^{\zeta}\zeta'^{-1}\phi_m\left(\zeta'\right)d\zeta'\right]^2}, \tag{6}$$

with $\zeta_0 = z_0/L$ and $\zeta_{0T} = z_{0T}/L$, where the surface roughness z_0 is defined as that height at which wind speed vanishes according to (4); z_{0T} corresponds to the surface skin temperature (i.e., the measurable radiative temperature). Notice that the assumption $k_m = k_h$ is not needed. Solving (6), the dimensionless parameter $\zeta = z/L$ is obtained for each hour; hence, friction velocity, temperature scale, surface heat flux, eddy diffusion coefficients, and viscous dissipation rate are all derived too, as will be seen below.

Before solving (6), two issues must be faced: the analytical form of the universal functions ϕ_m and ϕ_h appearing in (4) and (5) and the values assigned to z_0 and z_{0T} in (6).

We have chosen the analytical form of the universal functions estimated by Högström (1988):

$$\phi_m(z/L) = \begin{cases}(1 - 19.3z/L)^{-1/4}, & -2 < z/L < 0\\ 1 + 6z/L, & 0 < z/L < 1\end{cases} \quad \text{and} \tag{7}$$

$$\phi_h(z/L) = \begin{cases}0.95(1 - 11.6z/L)^{-1/2}, & -2 < z/L < 0\\ 0.95 + 7.8z/L, & 0 < z/L < 1.\end{cases} \tag{8}$$

Very similar results have obtained with the use of the Businger and Dyer universal functions and therefore they are not shown.

Concerning the value given to z_0, Sutton et al. (1978) estimated values of z_0 between 0.1 and 1 cm for the Viking missions, whereas Haberle et al. (1993) indicated that a better upper limit could be 10 cm. For the PF mission, Larsen et al. (2002) derived the value of z_0 from the images of the surroundings of the lander as reported in Science (1997) and assigned a value of 1 cm after applying Lettau's formula (Lettau 1969). Nevertheless, based on the existing uncertainties, values of 0.1, 1, and 10 cm have been used in this work.

The last matter is related to the use of a molecular sublayer and, consequently, the value given to z_{0T}. In keeping with the composition of the air and the fact that $\rho_{\text{Mars}}/\rho_{\text{Earth}} \sim 10^{-2}$, molecular kinematic viscosity and molecular thermal diffusivity [both on the order of 10^{-3} m^2 s^{-1} on Mars; Sutton et al. (1978)] are two orders of magnitude higher on Mars than on Earth. The molecular sublayer will definitely be more in evidence in Mars, and its inclusion becomes more necessary be-

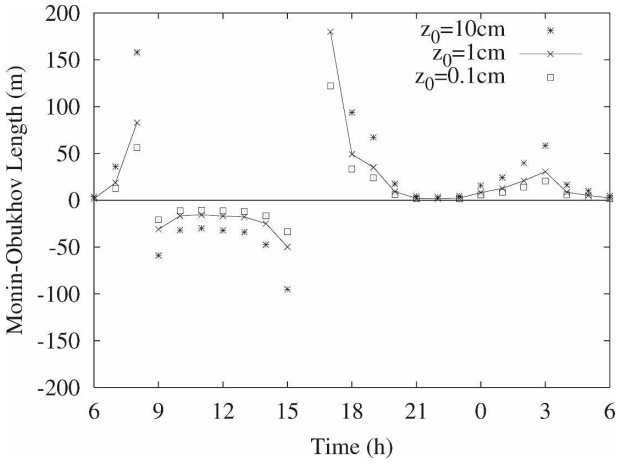

FIG. 3. Diurnal evolution of the Monin–Obukhov length for the different proposed surface roughness values (PF mission, sols 25–26).

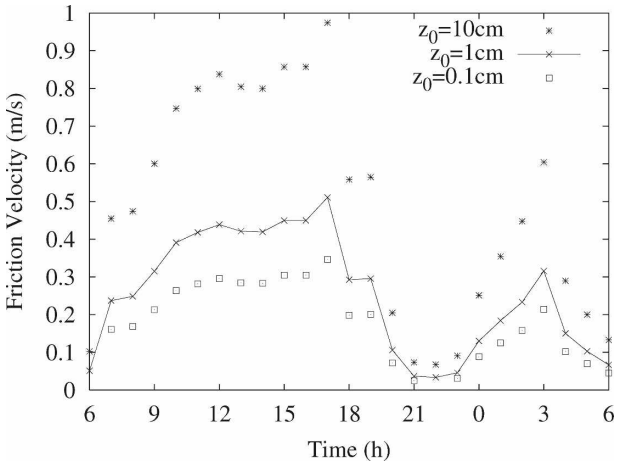

FIG. 4. Diurnal evolution of friction velocity for the different proposed z_0 values (PF mission, sols 25–26).

cause similarity theory neglects molecular processes. A parameterization for this sublayer corresponding to surfaces with bluff impermeable elements will be proposed.

4. Results

First of all, results without the inclusion of the molecular sublayer are shown, assuming $z_{0T} = z_0$. Diurnal evolutions, dependences on the parameter z_0, and comparisons to other Martian papers are presented. Then, the molecular sublayer is included and the affected magnitudes are described. Finally, a comparison between orders of magnitude on Earth and on Mars is carried out for all the obtained parameters.

a. Case study I: No molecular sublayer

1) MONIN–OBUKHOV LENGTH

By solving the implicit Eq. (6) for each of the different values of z_0, the Monin–Obukhov length is obtained. By definition, L is negative under local static instability conditions. As can be seen in Fig. 3, over much of the daytime, when convection is very strong, its value becomes negative and close to zero (about −25 m for $z_0 = 1$ cm). At night, it becomes positive following the nocturnal local static stability. Around sunrise and sunset, the values of L seem to diverge. However, this behavior has no physical meaning because the obtained surface heat flux vanishes momentarily because the ground temperature equals the temperature at the height of the sensor. Therefore, the applicability of the Monin–Obukhov similarity theory for thermally stratified surface layers is no longer valid given that the surface layer is not thermally stratified in the first meter at that moment. This magnitude has been found to vary less than 20% when it has been determined under the extreme ground temperature scenarios.

Another important aspect is the increase in the value of L with z_0 (also displayed in Fig. 3). Because the absolute value of L is thought to be proportional to the height of the layer in which shear effects dominate buoyancy effects, the higher the terrain roughness becomes, the more important the shear effects, and consequently L, are.

The hyperbolic diurnal behavior and the order of magnitude match with those found by Sutton et al. (1978) and Tillman et al. (1994) in the Viking Lander 2 data for early summer and early spring, respectively.

2) FRICTION VELOCITY AND SURFACE HEAT FLUX

Once the dimensionless parameter $\zeta = z/L$ is obtained from (6), it is straightforward to derive the diurnal evolution for u_* by integrating (4).

Friction velocity represents the turbulent vertical exchange of horizontal momentum between the ground and the first few meters of the atmosphere. Thus, it is reasonable to expect maximum values when the 1.3-m wind peaks because the shear becomes maximum. This behavior is observed in Fig. 4, where u_* follows the evolution of the mean wind (see Fig. 1), although it is modulated by the prevailing stability. It can also be noticed that friction velocity grows with the parameter z_0 because more horizontal momentum is lost to the ground if the surface becomes rougher. Its magnitude is on the order of 0.1 m s^{-1} for the proposed values of z_0, and its values vary less than 5% when the extreme scenarios for the ground temperature are imposed. Similar quantitative results have been obtained by Sutton et al. (1978), Tillman et al. (1994), and Haberle et al. (1993)

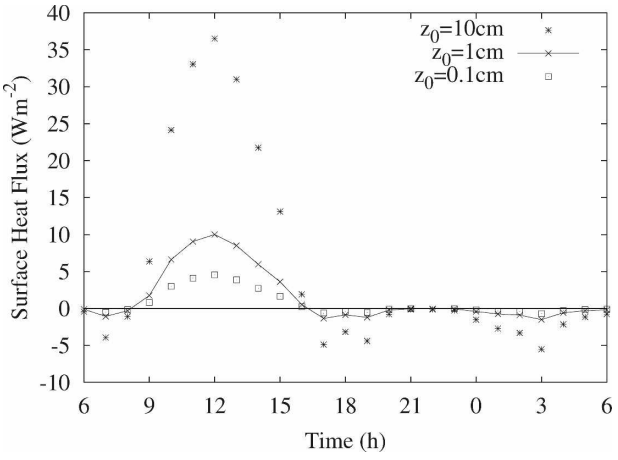

FIG. 5. As in Fig. 4, but for dynamic surface heat flux.

for Viking Landers 1 and 2 in the early summer. However, the second peak is not so evident in these works.

The temperature scale T_* has been obtained by integrating (5). This parameter represents the typical eddy temperature fluctuations in the surface layer. In this work, values of T_* on the order of 1 K for convective daytime have been obtained. This magnitude is consistent with the temperature fluctuations observed by the PF lander because changes on the order of 1 K could be detected in minutes. As an alternative, T_*^{alt} has also been calculated using the above derived z/L values and the in situ temperature measurements at 0.52, 0.77, and 1.3 m. Assuming neutral stability conditions, $T_*^N = kz\partial T/\partial z$ has been calculated from these three heights. Taking advantage of the obtained $\phi_h(z/L)$ values [see (8) with z/L calculated via (6)], it is a good approximation to state that $T_*^{\text{alt}} = T_*^N/\phi_h(z/L)$ [see (5)]. The match between the scale temperature values determined by this approach and the ones previously obtained is quite good. In both cases, the order of magnitude under stable conditions is around 0.1 K, whereas under instability it is around 1 K (with maximum values around 5 K).

Instead of representing its diurnal evolution, we have shown the dynamic surface heat flux

$$H_0 = -\rho c_p u_* T_* \tag{9}$$

in Fig. 5. It is positive (directed upward) during the daytime when local static instability conditions prevail because the ground is warmer than the first few meters of the atmosphere, and it is negative during the night, when the first meters become statically stable. The flux is maximum at noon, ~10 W m^{-2} for $z_0 = 1$ cm, because although friction velocity reaches its maximum later (Fig. 4), the difference between ground and sensor temperature (Fig. 2) causes T_* to peak at this time. The rest of the day it remains close to zero because of the attenuation of turbulence (u_* diminishes) and the decrease of the difference between air and ground temperature. As in the case of Monin–Obukhov length, surface heat flux varies less than 20% in the extreme scenarios.

Dynamic surface heat flux increases with the surface roughness as u_* and T_* do. Similar results have been yielded by other authors for Viking mission, with maxima about ~10 W m^{-2}. With regard to the PF mission, Savijärvi (1999) estimated maxima of 14 W m^{-2}.

3) TURBULENT VISCOUS DISSIPATION RATE AND EDDY DIFFUSIVITY COEFFICIENTS

Based on the similarity theory, any magnitude involving no more fundamental dimensions than time, longitude, and temperature is a unique function of the parameter $\zeta = z/L$ when made dimensionless by the fundamental scales z, u_*, and T_*. As we know, the values of these scales, as well as the value of $\zeta = z/L$, the eddy diffusivity coefficients for heat and momentum, and turbulent viscous dissipation rate, will be derived.

Starting with the diffusivity coefficients k_h and k_m and noting that their units are m^2 s^{-1}, the term that makes the diffusivity coefficients dimensionless must be $1/\kappa z u_*$. Hence,

$$k_m/\kappa z u_* = F(\zeta) \quad \text{and}$$

$$k_h/\kappa z u_* = G(\zeta),$$

where κ is the von Kármán constant, and F and G are unknown functions of the parameter ζ. Taking into account that

$$\overline{u'w'} = -u_*^2 = -k_m \frac{\partial U}{\partial z} = -k_m \frac{u_*}{kz}\phi_m(\zeta) \quad \text{and}$$

$$\overline{T'w'} = -u_* T_* = -k_h \frac{\partial T}{\partial z} = -k_h \frac{T_*}{kz}\phi_h(\zeta),$$

where (2), (3), (4), and (5) have been used, the following relations are yielded for F and G:

$$F(\zeta) = \phi_m^{-1}(\zeta) \quad \text{and}$$

$$G(\zeta) = \phi_h^{-1}(\zeta),$$

with ϕ_m and ϕ_h given by (7) and (8). Eventually, the next relationships are derived for the eddy diffusivity coefficients:

$$\frac{kzu_*}{k_m} = \phi_m \quad \text{and} \tag{10}$$

$$\frac{kzu_*}{k_h} = \phi_h. \tag{11}$$

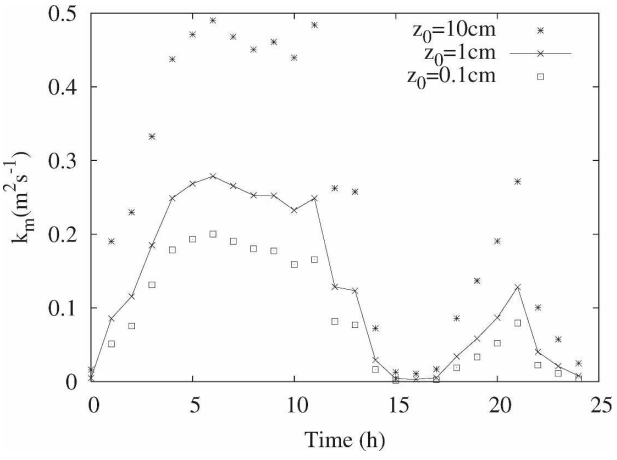

FIG. 6. Diurnal evolution of the 1.3-m eddy diffusion coefficient for momentum for the different proposed z_0 values (PF, sols 25–26).

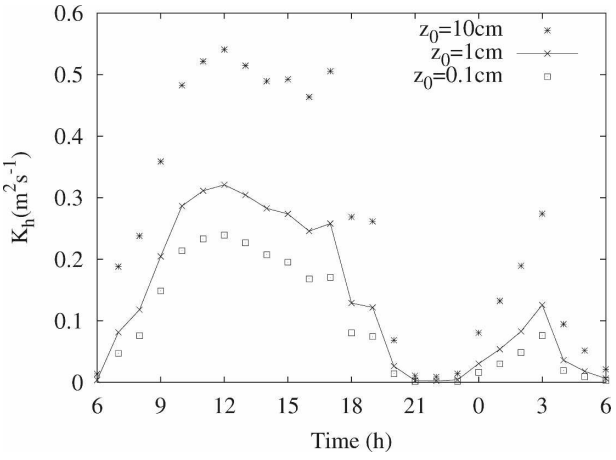

FIG. 7. As in Fig. 6, but for heat.

These parameters measure how efficient the atmosphere is at transporting momentum and heat via turbulent vertical fluxes. It is expected that the higher turbulent fluxes correspond to the higher value this parameter takes. This behavior, at 1.3-m height, is displayed in Figs. 6 and 7, where these coefficients tend to follow the friction velocity (Fig. 4). By construction, k_h is slightly higher than k_m in accordance with the universal functions employed, and their values are on the order of 0.1 $m^2\,s^{-1}$ (less than 5% of the variation found in the extreme scenarios). Thus, turbulent diffusion is two orders of magnitude more efficient than molecular diffusion, given that both molecular kinematic viscosity and molecular thermal diffusivity are on the order of 10^{-3} $m^2\,s^{-1}$.

We have also estimated values of k_m and k_h using the one-dimensional boundary layer model (Savijärvi et al. 2004) and found that simulated values are slightly higher at 1.3 m, although the order of magnitude is the same.

The turbulent viscous dissipation rate has been derived similarly. It is given in units of $m^2\,s^{-3}$, which implies that the dimensionless term that depends on ζ has to be

$$\frac{kz\epsilon}{u_*^3} = f(\zeta). \tag{12}$$

The analytical relationship between these two dimensionless parameters cannot be directly obtained as in the case of the diffusivity coefficients. However, Wyngaard and Coté (1971) yielded an empirical relation:

$$\frac{kz\epsilon}{u_*^3} = \begin{cases} (1 + 0.5(z/L)^{2/3})^{3/2}, & \text{where} \quad z/L > 0, \\ [1 + 2.5(z/L)^{3/5}]^{3/2}, & \text{where} \quad z/L < 0. \end{cases} \tag{13}$$

Making use of this relationship, values of ϵ are estimated. The turbulent viscous dissipation rate represents the conversion of turbulent kinetic energy into heat. As can be seen in Fig. 8, the turbulent viscous dissipation rate peaks at the same time as the friction velocity and behaves similarly. This is because $f(\zeta)$, in which buoyancy effects are considered via L, does not significantly change the shape of u_*. The physical cause lies in the fact that shear and dissipation are usually the dominant terms under stable conditions. Alternatively, under instability, buoyancy and turbulent transport, which are also important, tend to balance each other (Wyngaard and Coté 1971). In both cases dissipation is virtually in accordance with the shear, presenting maximum values around 0.1 $m^2\,s^{-3}$ during the daytime for z_0 = 1 cm, whereas at night it comes close to zero. The variation of this magnitude under the extreme ground temperature scenarios is lower than 5%. It is fair to say that the validity of (13) on Mars presents uncertainties. Until specific experiments can be conducted to measure the importance of each of the terms (shear, buoyancy, transport, and dissipation) of the turbulent kinetic energy, it will not be possible to assure that the balances previously mentioned are met. Nevertheless, it can be expected that they will be met.

b. Case study II: Inclusion of a molecular sublayer

The necessity of including the molecular sublayer in the similarity theory will be discussed. Those parameters that turn out to be affected by its inclusion will be highlighted, with explanations of how and why they have changed.

1) NEED FOR A MOLECULAR SUBLAYER

Molecular kinematic viscosity and molecular thermal diffusivity are on the order of 10^{-3} $m^2\,s^{-1}$ on Mars.

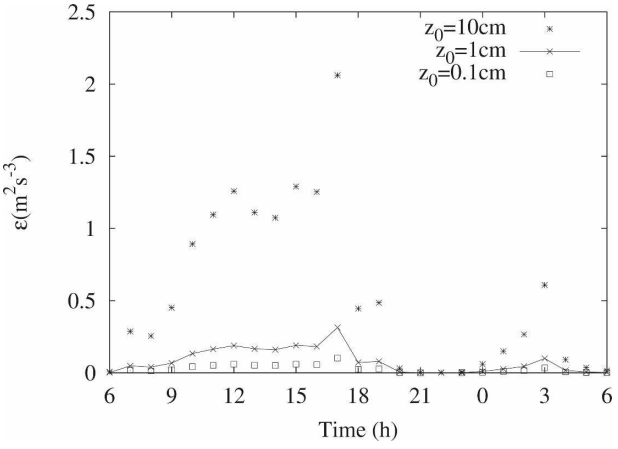

FIG. 8. Diurnal evolution of the 1–3 m viscous dissipation rate for the different proposed z_0 values (PF mission, sols 25–26).

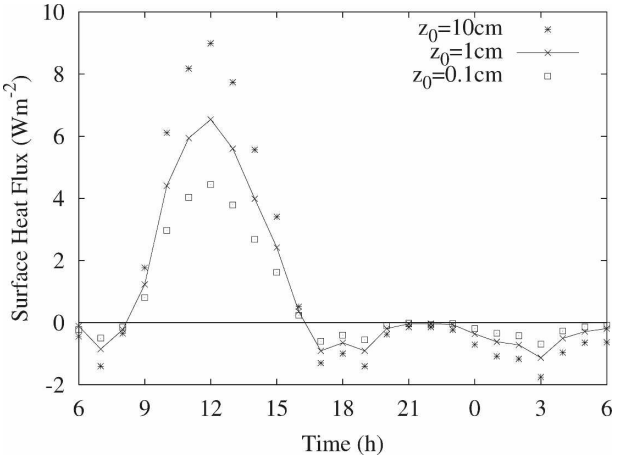

FIG. 9. Surface heat flux estimated with the inclusion of the molecular sublayer (PF mission, sols 25–26).

Taking into account that we have found eddy-transfer coefficients to be on the order of 10^{-1} m^2 s^{-1}, only two orders of magnitude separate the mechanisms on Mars. Because similarity theory neglects molecular diffusion, we have followed the approach used by Zilitinkevich (1970) and incorporated the molecular sublayer into the surface layer similarity theory by assuming a relation for z_0/z_{0T}. The difference between these two parameters tends to be greater for flow over bluff roughness elements (Hignett 1994), which makes its inclusion on Mars even more important.

The parameterization developed by Brutsaert (1982) will be used. With the aid of dimensional analysis and experiments, Brutsaert estimated the next relation for surfaces with bluff impermeable elements:

$$\ln\left(\frac{z_0}{z_{0T}}\right) = 7.3k\mathrm{Re}_0^{0.25}\mathrm{Pr}^{0.5} - 5k, \qquad (14)$$

where k is the von Kármán constant, $\mathrm{Re}_0 = z_0 u_*/\nu$ the roughness Reynolds number (where ν represents the kinematic viscosity), and Pr the Prandtl number. Different parameterizations can be found in the literature for other type of soils, although this one is expected to represent more accurately the Martian soil.

2) RESULTS

We have found that magnitudes directly related to z_{0T}—that is, the temperature scale through

$$T_* = \frac{k[T(z) - Tg]}{\displaystyle\int_{\zeta_{0T}}^{\zeta} \zeta'^{-1}\phi_h(\zeta')\,d\zeta'} \qquad (15)$$

and the dynamic surface heat flux through (9)—are sensitively affected by the inclusion of the molecular sublayer. Nevertheless, friction velocity and hence both turbulent viscous dissipation rate and eddy-transfer diffusivity coefficients are not. This behavior is reasonable because in this sublayer only molecular transfer is important for heat, whereas for momentum, in addition to the molecular transport, pressure fluctuations are very relevant so the net effect on the transport of momentum is less noticeable (Zeng and Dickinson 1998).

The main consequences found with the inclusion of the molecular sublayer are (i) a decrease of heat flux values for a given difference between air temperature and surface skin temperature and (ii) a reduction of z_0 dependence (z_{0T} lies in the range 10^{-3}–10^{-4} m for all z_0 values). Both aspects can be observed in Fig. 9 when it is compared to the values obtained without the inclusion of the molecular sublayer (see Fig. 5).

Similar results have been obtained for Viking missions by Sutton et al. (1978) and Haberle et al. (1993) when a molecular sublayer was used. In both cases, the principal effect of adding a molecular sublayer was to reduce the influence of z_0 on the heat fluxes, although for low values of z_0 the surface heat flux in Sutton et al. (1978) did not decrease (whereas it did for larger values of z_0). Tillman et al. (1994) assumed the same z_{0T} for all z_0 values, after having parameterized z_{0T} in a way similar to our method.

c. *Earth turbulent scales versus Martian turbulent scales*

In this section we shall compare the order of magnitude of the Martian parameters obtained here to those typically found on Earth, highlighting the main differences between both planets.

We start with the Monin–Obukhov length. Values of

TABLE 1. Values for the molecular and turbulent diffusion coefficients on Mars and on Earth; k_m and k_h represent turbulent diffusion coefficients for momentum and heat, respectively, at around 1.3 m. The kinematic molecular viscosity is represented by ν and the thermal molecular diffusivity by κ.

	ν ($m^2 s^{-1}$)	κ ($m^2 s^{-1}$)	k_m ($m^2 s^{-1}$)	k_h ($m^2 s^{-1}$)
Mars	$\sim 10^{-3}$	$\sim 10^{-3}$	$\sim 10^{-1}$	$\sim 10^{-1}$
Earth	$\sim 1.5 \times 10^{-5}$	$\sim 2 \times 10^{-5}$	~ 1–10^1	~ 1–10^1

L have been found to range between 0 and 100 m. These values also correspond to those typically found on Earth. That is, the height of the surface layer fits on both planets. Additionally, we have derived values around 0.1 m s^{-1} for the friction velocity, which turn out to be of similar magnitude to those on Earth (André et al. 1978).

Concerning the surface dynamic heat flux, maximum values around 10 W m^{-2} have been obtained. In desert environments, like the Gobi desert (Hartmann 1994), maximum values are one order of magnitude higher. This is due to the lower Martian atmospheric density, given that $\rho_{\text{Mars}}/\rho_{\text{Earth}} \sim 10^{-2}$ and that the specific heat capacities c_p are on the same order on both planets (around 730 J K^{-1} kg^{-1} on Mars and 1004 J K^{-1} kg^{-1} on Earth). According to the definition of H_0 in (9), and noticing that friction velocities have the same magnitude on both planets, we conclude that maximum values of the temperature scale T_* can reach one order of magnitude higher on Mars (remember that maximum H_0 values are one order of magnitude higher on Earth and that the term ρc_p is two orders of magnitude higher on Earth). Actually, values around 5 K have been found for T_* in this paper, whereas values between 0.1 and 1 K are typical for Earth. The difference can be explained as follows: surface energy budget is almost driven by radiation and virtually balanced by heat conduction in the soil (latent and sensible fluxes are much smaller in magnitude). In addition, the Martian ground presents low values of thermal inertia. Both aspects cause Martian ground to warm and cool as much as 80 K daily. Because air from above cannot follow the soil temperature evolution so rapidly (because of low atmospheric density), large temperature gradients are created, resulting in higher temperature scales.

Finally, the efficiency of both molecular and turbulent diffusion will be treated. Table 1 contains values of molecular and turbulent diffusion coefficients for both heat and momentum on both planets, with terrestrial values of k_m and k_h taken from Stull (1988) and values of the Martian eddy-diffusion coefficients at 1.3 m derived from this study. It can be seen that turbulent diffusion is five or six orders of magnitude more effective than molecular diffusion on Earth. However, this behavior is different on Mars because turbulent diffusion is only two orders of magnitude more effective than molecular diffusion.

5. Discussion and conclusions

Diurnal evolutions of Monin–Obukhov length, friction velocity, dynamic surface heat flux, eddy-transfer coefficients, and turbulent viscous dissipation rate have been determined for one complete PF Martian sol. Neither diurnal evolutions of the mentioned parameters nor values of turbulent viscous dissipation rate and eddy-transfer coefficients had been available from in situ wind and temperature measurements for the PF.

The reason might lie in the problem experienced by the wind sensor located on the PF lander. Because of overheating of the sensor wire segments, from which wind speed was to be derived, in situ wind data are not available in the Planetary Data Science dataset. However, the gas-temperature thermocouple had been expected to provide a valid representation of the unheated wire temperature. Using this means, we received wind data covering from 0600 sol 25 to 0600 sol 26. The in situ top height–measured temperature over the same period as the wind and the simulated ground temperature complete the set of inputs.

Two reliable extreme scenarios have been created for the ground temperature. It has been found that friction velocity, turbulent diffusivity coefficients, and turbulent viscous dissipation rate vary less than 5% regarding to the shown reference values, whereas the Monin–Obukhov length and surface heat flux vary around 20%. In all cases, the order of magnitude of these magnitudes remains unchanged.

An interval of 0.1 to 10 cm for the surface roughness has been taken on the basis of the values found in the bibliography. We have calculated values of the Monin–Obukhov length in the range of 0 to 100 m as well as a typical hyperbolic behavior. On Earth, the magnitude of L matches the one found on Mars. Thus, the height of the surface layer is expected to be similar on both planets.

Friction velocity values have been found to be on the order of 0.1 m s^{-1} as on Earth. Such velocity grows with z_0 because more horizontal momentum is lost to the ground if the surface becomes rougher. The value of this parameter is very important when considering saltation of grains.

The temperature scale and surface dynamic heat flux show remarkable differences between Mars and Earth. Temperature fluctuations of about 8 K were measured by the PF lander in the turbulent time scale, that is, in

seconds or few minutes. Accordingly, we have found maximum values of T_* around 5 K. Typical eddy temperature fluctuations on Earth are on the order of 0.1 K. On the other hand, maximum values around 10 W m^{-2} for $z_0 = 1$ cm for the surface heat flux have been obtained, whereas in terrestrial deserts peaks on the order of 400–500 W m^{-2} can be found. Both T_* and H_0 show different values on both planets because of some unique Martian characteristics (by unique we mean that they are not met on Earth). Because the net radiation that reaches the Martian soil is almost the same as on Earth, and sensible and latent fluxes are much lower on Mars (because of low atmospheric density and a virtual absence of water vapor), the heat conduction in the soil becomes very important [the thermal effect of the radiation at the surface has been studied in Zorzano and Vázquez (2006) and Vázquez et al. (2007)]. In addition, the thermal inertia is low. This all results in large ground temperature fluctuations (around 80 K through one sol). Because the air atmospheric density is very low, the first few meters of Martian air cannot be heated efficiently; thus, they do not follow the ground temperature diurnal evolution. Consequently, large temperature gradients are created and therefore higher values of T_* are observed.

Concerning the turbulent viscous dissipation rate, values between 10^{-4} and 10^{-1} $m^2 s^{-3}$ have been determined, which is in accordance with the range found in the terrestrial surface layer. This parameter has been obtained by supposing that shear and dissipation are almost in balance the whole day. This means that only these two terms become important under stability, whereas under instability, buoyancy and transport, which are also relevant in magnitude, tend to balance each other. This statement cannot be assured for the MSL until specific experiments are conducted.

The eddy-transfer coefficients for both momentum and heat have been found to be $\sim$0.1 $m^2 s^{-1}$ at 1.3 m during daytime. Both parameters present maximum values corresponding to maximum shear. Values around 1–10^1 $m^2 s^{-1}$ are typical for Earth. Noticing that on Mars both molecular kinematic viscosity and thermal diffusivity are around 10^{-3} $m^2 s^{-1}$, only two orders of magnitude separate molecular diffusion from turbulent diffusion on Mars, whereas on Earth turbulent diffusion is five or six orders of magnitude more efficient than molecular exchanges.

The need to include a molecular sublayer in the similarity theory has been explained. Martian density has a low atmospheric value which, along with the bluff roughness elements that form the Martian soil, cause the difference between z_0 and z_{0T} to become greater. We have used the parameterization proposed by Brutsaert (1982) and have found that only the temperature scale and surface dynamic heat flux are affected by its inclusion. This result was expected because only molecular transfer is important for heat in this sublayer, whereas for momentum, in addition to molecular transport, pressure fluctuations are very relevant. The main consequences of the inclusion of the molecular sublayer are a decrease in heat flux values (although not drastically) for a given difference between air temperature and ground temperature and a reduction of the z_0 dependence.

Uncertainties related to the use of the Monin–Obukhov similarity have been described. The validity of the universal functions for heat and momentum and Eq. (12) should be tested on the MSL. However, until wind (horizontal and vertical component) and temperature can be monitored simultaneously at several heights with a high enough sampling rate (>1 Hz), the use of the Monin–Obukhov similarity is essential in research concerning the MSL.

Acknowledgments. We thank both the firm Arquimea S.L. and the MEC project CGL2005–06966-C07–04 for their financial support. We also thank Prof. Sävijärvi (University of Helsinki) for his advice on the use of his model and Prof. Jim Murphy (New Mexico University) for providing us with wind data and helping us in the preparation of this paper. Prof. Luis Vázquez thanks the partial support from the Dirección General de Investigación of Spain, under Grant MTM2005–05573. Finally, we thank the MEC's project ESP2007-30487-E "El Ciclo de la humedad en la superficie de Marte" and the referees for their useful advise for improving the paper.

REFERENCES

André, J. C., G. De Moor, P. Lacarrère, G. Therry, and R. du Vachat, 1978: Modeling the 24-hour evolution of the mean and turbulent structure of the planetary boundary layer. *J. Atmos. Sci.,* **35,** 1861–1883.

Arya, P., 2001: *Introduction to Micrometeorology.* Academic Press, 420 pp.

Brutsaert, H., 1982: Exchange processes at the earth–atmosphere interface. *Engineering Meteorology,* E. Platte, Ed., Elsevier, 319–369.

Christensen, P., and Coauthors, 2001: Mars Global Surveyor Thermal Emission Spectrometer experiment: Investigation description and surface science results. *J. Geophys. Res.,* **106** (E10), 23 823–23 871.

Golombek, M., and Coauthors, 1997: Overview of the Mars Pathfinder Mission and assessment of landing site predictions. *Science,* **278,** 1743–1748.

Haberle, R., H. Houben, R. Hertenstein, and T. Herdtle, 1993: A boundary layer model for Mars: Comparison with Viking lander and entry data. *J. Atmos. Sci.,* **50,** 1544–1559.

Hartmann, D., 1994: *Global Physical Climatology.* Academic Press, 411 pp.

Hess, S., R. Henry, C. Leovy, J. Tillman, and J. Ryan, 1977: Meteorological results from the surface of Mars—Viking 1 and 2. *J. Geophys. Res.,* **82,** 4559–4574.

Hignett, P., 1994: Roughness lengths for temperature and momentum over heterogeneous terrain. *Bound.-Layer Meteor.,* **68,** 225–236.

Högström, U., 1988: Non-dimensional wind and temperature profiles in the atmospheric surface layer: A re-evaluation. *Bound.-Layer Meteor.,* **42,** 55–78.

Johnson, J., W. Grundy, and M. Lemmon, 2003: Dust deposition at the Mars Pathfinder landing site: Observations and modeling of visible/near-infrared spectra. *Icarus,* **163,** 330–346.

Larsen, S., H. Jørgensen, L. Landberg, and J. Tillman, 2002: Aspects of the atmospheric surface layers on Mars and Earth. *Bound.-Layer Meteor.,* **105,** 451–470.

Lettau, H., 1969: Note on aerodynamic roughness-parameter estimation on the basis of roughness-element description. *J. Appl. Meteor.,* **8,** 828–832.

Määttänen, A., and H. Savijärvi, 2004: Sensitivity tests with a one-dimensional boundary-layer Mars model. *Bound.-Layer Meteor.,* **113,** 305–320.

Monin, A. S., and A. M. Obukhov, 1954: Osnovnye zakonomernosti turbulentnogo peremeshivanija v prizemnon sloe atmosfery (Basic laws of turbulent mixing in the atmosphere near the ground). *Trudy Geofiz. Inst. AN SSSR,* **24,** 163–187.

Putzig, N., M. Mellon, K. Kretke, and R. Arvidson, 2005: Global thermal inertia and surface properties of Mars from the MGS mapping mission. *Icarus,* **173,** 325–341.

Savijärvi, H., 1991: A model study of the PBL structure on Mars and the Earth. *Beitr. Phys. Atmos.,* **64,** 219–229.

——, 1999: A model study of the atmospheric boundary layer in the Mars Pathfinder lander conditions. *Quart. J. Roy. Meteor. Soc.,* **125,** 483–493.

——, and T. Siili, 1993: The Martian slope winds and the nocturnal PBL jet. *J. Atmos. Sci.,* **50,** 77–88.

——, A. Määttänen, J. Kauhanen, and A. Harri, 2004: Mars Pathfinder: New data and new model simulations. *Quart. J. Roy. Meteor. Soc.,* **130,** 669–683.

Schofield, J., and Coauthors, 1997: The Mars Pathfinder Atmospheric Structure Investigation/Meteorology (ASI/MET) experiment. *Science,* **278,** 1752–1758.

Science, 1997: Mars Pathfinder images. *Science,* **278,** 1734–1742.

Stull, R., 1988: *An Introduction to Boundary Layer Meteorology.* Springer, 670 pp.

Sutton, J., C. Leovy, and J. Tillman, 1978: Diurnal variations of the Martian surface layer meteorological parameters during the first 45 sols at two Viking lander sites. *J. Atmos. Sci.,* **35,** 2346–2355.

Tillman, J., L. Landberg, and S. Larsen, 1994: The boundary layer of Mars: Fluxes, stability, turbulent spectra, and growth of the mixed layer. *J. Atmos. Sci.,* **51,** 1709–1727.

Vázquez, L., M. Zorzano, and S. Jimenez, 2007: Spectral information retrieval from integrated broadband photodiode Martian ultraviolet measurements. *Opt. Lett.,* **32,** 2596–2598.

Wyngaard, J., and O. Coté, 1971: The budgets of turbulent kinetic energy and temperature variance in the atmospheric surface layer. *J. Atmos. Sci.,* **28,** 190–201.

Zeng, X., and R. Dickinson, 1998: Effect of surface sublayer on surface skin temperature and fluxes. *J. Climate,* **11,** 537–550.

Zilitinkevich, S., 1970: *Dynamics of the Atmospheric Boundary Layer.* Gidrometeoizdat, 282 pp.

Zorzano, M., and L. Vázquez, 2006: Remote temperature retrieval from heating or cooling targets. *Opt. Lett.,* **31,** 1420–1422.